metals

MDPI

Article

Study on Performance of PVD AlTiN Coatings and AlTiN-Based Composite Coatings in Dry End Milling of Hardened Steel SKD11

Lulu Jing [1,*], Ming Chen [2] and Qinglong An [2]

[1] School of Mechanical Engineering, University of Shanghai for Science and Technology, Shanghai 200093, China
[2] School of Mechanical Engineering, Shanghai Jiao Tong University, Shanghai 200030, China; mchen@sjtu.edu.cn (M.C.); qlan@sjtu.edu.cn (Q.A.)
* Correspondence: jinglulu56@163.com

Abstract: Dry milling of hardened steel is an economical and environmentally friendly machining process for manufacturing a mold and die. Advances in coating technology makes the dry milling a feasible approach instead of a traditional grinding process. However, the cutting condition is particularly severe in a dry machining process. High-performance coating is desired to meet the requirement of green and highly efficient manufacturing. This study concerned the performance of AlTiN-based coatings. The effect of Al content, and the AlTiN composite coating on the cutting performance of tools are investigated in terms of friction force at the tool–chip interface, specific cutting energy, cutting temperature on the machined surface, tool wear pattern and mechanism, and surface integrity. The results show that advanced AlTiN-based coatings reduce the force and cutting energy and protect the cutters from the high cutting temperature effectively. The main wear mechanisms of the coated tools are adhesive wear, chipping induced by fatigue fracture and abrasive wear. In general, the dry milling of hardened steel with AlTiN-based coatings gains a quite satisfactory surface quality. Furthermore, AlTiN-WC/C hard-soft multilayer coating performs well in reducing cutting force, preventing adhesion wear and isolating the cutting heat, being suitable for dry milling of hardened SKD11.

Keywords: dry end milling; hard cutting; AlTiN coating; AlTiN-WC/C multilayer coating

check for updates

Citation: Jing, L.; Chen, M.; An, Q. Study on Performance of PVD AlTiN Coatings and AlTiN-Based Composite Coatings in Dry End Milling of Hardened Steel SKD11. *Metals* **2021**, *11*, 2019. https://doi.org/10.3390/met11122019

Academic Editor: Emin Bayraktar

Received: 15 November 2021
Accepted: 10 December 2021
Published: 14 December 2021

Publisher's Note: MDPI stays neutral with regard to jurisdictional claims in published maps and institutional affiliations.

Copyright: © 2021 by the authors. Licensee MDPI, Basel, Switzerland. This article is an open access article distributed under the terms and conditions of the Creative Commons Attribution (CC BY) license (https://creativecommons.org/licenses/by/4.0/).

1. Introduction

Hardened steel SKD11with a hardness up to 60–62 HRC is widely utilized in the producing of dies, precision gauges, spindle, jigs and fixtures due to high toughness and excellent wear resistance [1,2]. On the other hand, it is considered as one of the difficult-to-cut materials [3].

The traditional approach to machine this hard steel is a grinding and electronic discharge machining (EDM) process. With the development in machine tools and cutting tools, to manufacture alloy steels in the fully hardened state becomes a cost-effective manufacturing process in the finishing machining of dies and molds [4]. Tools always bear high mechanical and thermal loads, which lead to the deterioration in cutting performance [5]. In the traditional cutting process, cutting fluid plays an essential role of lubrication and cooling. However, the usage of cutting fluid causes several problems: the increase of manufacturing costs, the pollution of the environment and the harm to operators [6]. Extensive studies have been conducted to improve this situation, such as minimum quantity lubrication (MQL) [7,8], environmentally friendly cutting fluids [9,10], and dry cutting [5,11].

The benefits for dry milling of hardened steel components are substantial in terms of reduced machining costs and lead time, protection of the environment and human

health [12,13]. If no cutting fluid is used in the milling of hardened steel, the cooling, lubrication and chip removal becomes particularly severe. The friction between the tool and chip increases, resulting in the increase of cutting force and cutting temperature [14]. To overcome these difficulties, heat-resistant tool materials and advanced coating materials have been developed [15].

Advances in coating techniques have promoted the spread of the dry machining [16,17]. Coating one or more layers of metal or non-metal compound films with high hardness and good wear resistance on the relatively soft tool substrate material greatly improves the mechanical properties of the tool [18]. By adding aluminum to TiN coatings, AlTiN coatings acquire higher hardness, advanced wear resistance and oxidation resistance at high temperatures [19,20]. The mechanical properties and crystal structure of AlTiN coatings are positively correlated to their Al content. With an appropriate aluminum concentration in the AlTiN coating, it is appropriate to form a hard and inert film at the tool-chip interface during cutting. This film not only prevents further oxidation of the coating, but also performs heat insulation [21].

AlTiN coating can be combined with other coatings to form multilayer coating, for instance AlTiN hard coating–soft coating. Each layer of coating has its own advantages, so that the composite coating has better comprehensive performance [22]. Soft coating is also named as self-lubricating coating. With excellent lubrication performance, it reduces the friction between the workpiece and the tool, prevent the generation of chip adhesion so as to improve the processing surface quality and prolong the tool life [23]. Tungsten carbide and carbon (WC/C)-based coating is a soft coating. Various studies are available regarding the anti-frictional behavior of WC/C coating [24,25]. However, little research has been reported on the application of WC/C coating on carbide tools in dry milling.

In addition, nanocomposite coatings have been developed and applied in machining with extreme conditions [26,27]. The AlTiN-based nanocomposite coatings have very high nanohardness and heat resistance, which could significantly improve the high temperature hardness, heat insulation property, thermal stability, and impact toughness [28]. The cutting speed and tool life could be improved significantly.

Various studies have conducted on WC/C coating and AlTiN based nanocomposite coatings and show their capacity in extreme machining condition. However, little research has paid attention to investigate their effects on the cutting performance in dry milling of hardened steel. In addition, although several studies investigated the effect of Al content in coating chemical compositions, the performance of AlTiN PVD coatings with different Al/Ti ratios during dry milling of hardened steel is seldom reported. This study aims to investigate and compare the performance of PVD AlTiN coatings with two different Al/Ti ratios, AlTiN-WC/C hard–soft composite coatings and AlTiN/Si3N4 nanocomposite coatings in dry end milling of hardened steel. Four kinds of different coatings are applied on cemented carbide cutters. The effects of the coatings on cutting performance of tools are investigated in terms of friction force at the tool–chip interface, specific cutting energy, cutting temperature on the machined surface, tool wear pattern and mechanism, and surface integrity.

2. Materials and Methods

2.1. Testing Materials

In the experiment, the workpiece of JIS SKD11 tool steel are used. Table 1 shows the properties and compositions of this material. SKD11 is a widely used cold-work tool steel, which has similar contents and properties as AISI D2 steel. The workpiece has been fully hardened and contains large amounts of carbides, which give an excellent resistance to wear, and has a fine tempered martensite microstructure with a hardness of 60 to 62 HRC.

Four kinds of coatings are deposited on milling cutter fabricated by cemented carbide H10F with the properties and compositions as shown in Table 2. The cutters have same geometrical parameters as shown in Table 3.

Table 1. Properties and composition of SKD11 steel.

Properties	Density 8400 kg/m^3		Young's Modulus 208 GPa		Poisson's Ratio 0.3		Hardness 60–62 HRC	
Compositions wt.%	C	Si	Mn	Cr	Mo	V	P<	S<
	1.40~1.60	0.40	0.60	11.00~13.00	0.80~1.20	0.20~0.50	0.03	0.03

Table 2. Properties and compositions of the cemented carbide H10F.

Properties	Hardness 1600 HV30	Bending Strength 4300 N/mm^2	Compressive Strength 6250 N/mm^2	Grain Size 0.8 μm
Compositions wt.%	W	C	Co	Cr
	80.99	9.78	8.83	0.4

Table 3. Cutting tool geometry and cutting parameters.

Geometric Parameters		**Cutting Parameters**	
Diameter	12 mm	Cutting speed	75 m/min
Cutter fluted	4	Feed rate	0.1 mm/tooth
Rake angle	10°	Axial depth	6 mm
Clearance angle	5°	Radial depth	0.3 mm
Helix angle	45°	Cooling fluid	Dry

Two types of AlTiN coatings with different Al contents are fabricated by a PVD ARC process. The mole Al/Ti ratios are 50:50 and 67:33, respectively. AlTiN/Si_3N_4 nanocomposite coatings are fabricated adopting LARC (lateral rotating ARC-cathodes) technology. Under the action of strong ions, nano-AlTiN crystals are embedded in the amorphous Si_3N_4, formed a honeycomb structure. AlTiN-WC/C multilayer coating are fabricated by depositing a layer of WC/C film on the AlTiN coating. This soft WC/C film has good lubrication performance, very low friction coefficient, and can prevent adhesion wear effectively. These coatings have shown their capacity in extreme machining condition. However, their effects on the cutting performance in dry milling of hardened still need to be revealed.

2.2. Milling Tests

Milling experiments are carried out on a MAHO MH600C CNC milling center under dry conditions. The travel range of the machine tool is defined as: longitudinal travel (*X*-axis) 600 mm, cross travel (*Y*-axis) 450 mm and vertical travel (*Z*-axis) 450 mm. The spindle rotational speed ranges from 20 to 4000 rpm. Cutting conditions are present in Table 3. The cutting parameters are selected based on industry recommendations and preparatory experiments. Due to high hardness and low thermal conductivity of the material, a moderate cutting speed is selected, so as to avoid excessive cutting heat and tool wear.

The cutting forces are measured using a four-component piezoelectric dynamometer Kistler 9272, with a multi-channel charge amplifier Kistler 5017NB, and the data acquisition system with a sampling frequency of 4 kHz. The measured force directions are set as follows, Fx is along the feed, Fy is normal to the feed and Fz is along the axial direction.

In addition, semi-artificial thermocouple method is used to measure the temperature of the cutting zone. A thin constantan wire is implanted between two SKD11 specimens and kept insulated from them. During milling, the constantan wire and SKD11 are cut off and form a thermal contact to generate voltage signals. The measurements are performed three times and the average value is adopted. The experimental setup of the end milling tests is present in Figure 1.

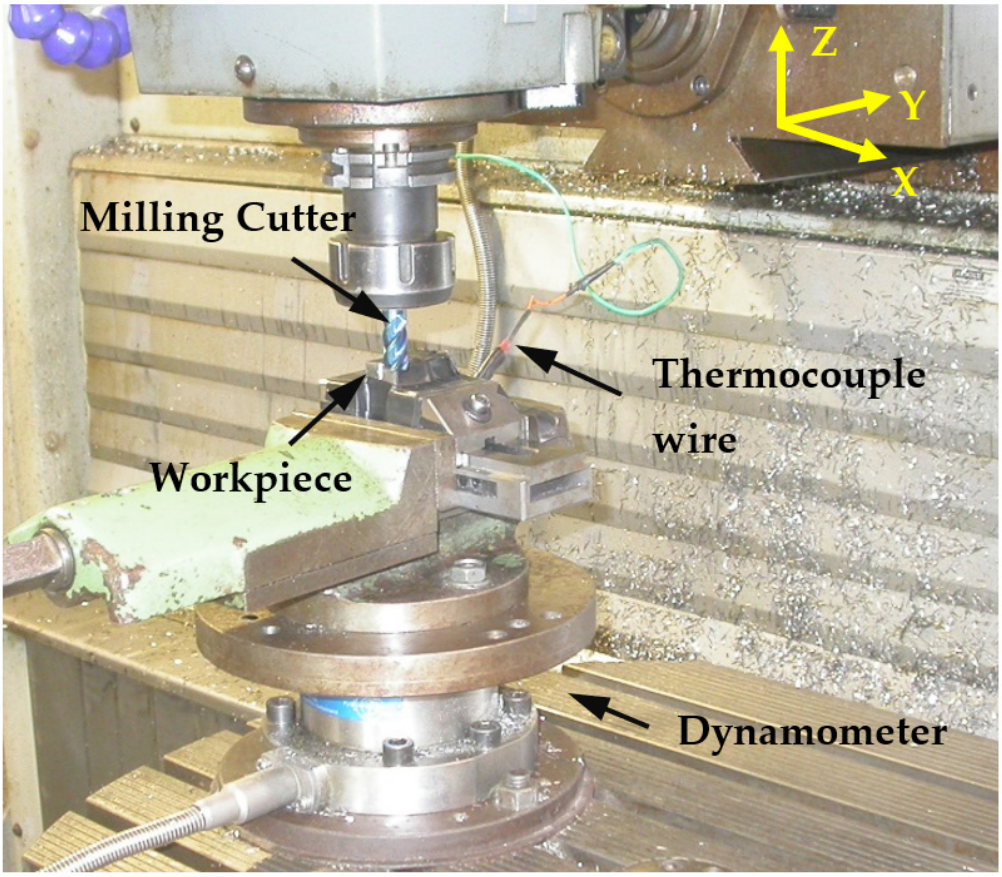


Figure 1. Experimental setup of dry end milling of SKD11.

For tool wear analysis, the cutter is taken off and observed every 0.8 m of cutting length. Tool edge morphology is recorded by a Nikon microscope and digital camera with 1 µm resolution. Scanning electron microscope (SEM) and energy-dispersive spectroscopy (EDS) analyses are performed on tool wear region to study the wear morphology and chemical composition by using a JSM-6460 SEM.

After the dry milling, specimens are cut from the workpiece, and cleaned using acetone alcohol. These specimens are polished metallographically. The changes in the hardness of the workpiece surface are measured using an Rockwell hardness tester with a load of 150 kg. Residual stresses are measured using an X350A X-ray diffraction system based on the dφψ-sin2ψplotting method. The stresses are calculated by measuring the change of crystal plane spacing under the action of residual stress by X-ray diffraction, which is a non-destructive method.

3. Results and Discussion

3.1. The Force Components and Specific Energy

End milling process is a complicated 3-D oblique cutting process. Due to the helical angle, cutting direction and undeformed chip layer varies along cutting edge [29]. Considering the shearing force and plowing force components, cutting force in milling could be expressed in differential equations as follows [30],

$$d\mathbf{F}(\phi, z) = [\mathbf{K}_c h(\phi, z) + \mathbf{K}_e] dz \quad (1)$$

where the $\mathbf{F}(\phi, z)$ is the cutting force, $\mathbf{K}_c$ is the shearing force coefficient, $\mathbf{K}_e$ is the plowing force coefficient. $h(\phi, z)$ is uncut chip thickness, ϕ is instant contact angle and z is the height of the milling cutter.

To investigate the influence of different coatings on the friction and pressure at the tool–chip interface on the rake face, the cutting force coefficients with reference to tool rake face need to be identified. The measured force components could be converted from the force components with reference to tool face as follows,

$$\begin{bmatrix} dF_x \\ dF_y \\ dF_z \end{bmatrix} = \begin{bmatrix} -\cos\phi & -\sin\phi & 0 \\ \sin\phi & -\cos\phi & 0 \\ 0 & 0 & 1 \end{bmatrix} \begin{bmatrix} \cos i & 0 & \sin i \\ 0 & 1 & 0 \\ -\sin i & 0 & \cos i \end{bmatrix} \begin{bmatrix} \cos\gamma_n & \sin\gamma_n & 0 \\ -\sin\gamma_n & \cos\gamma_n & 0 \\ 0 & 0 & 1 \end{bmatrix} \begin{bmatrix} dF_{r1} \\ dF_{r2} \\ dF_{r3} \end{bmatrix} \quad (2)$$

where ϕ is instant contact angle, γ_n is the normal rake angle measured in the plane perpendicular to cutting edge, which can be determined with rake angle γ_0 and inclined angle which is equal to the helical angle i.

$$\tan\gamma_n = \tan\gamma_0 \cos i \quad (3)$$

Figure 2 shows the cutting force coefficients on the rake face, where Krc is the friction force coefficient and Knc is the normal force coefficient. These two force coefficients of different tools exhibit the similar trend as each other. The order of cutting force coefficients from large to small is AlTiN (50:50) coating, AlTiN/Si3N4 coating, AlTiN (67:33) coating and AlTiN-WC/C coating. The AlTiN-WC/C multilayer coatings significantly reduced the cutting force by nearly 65%, 55% and 40% than that of AlTiN (50:50) coating, AlTiN/Si_3N_4 coating and AlTiN (67:33) coating, respectively. Figure 3 gives the specific cutting energy consumed in cutting process by different cutters with the tested cutting parameters. The highest cutting energy is produced by AlTiN (50:50) coating, followed by AlTiN/Si_3N_4 coating, AlTiN (67:33) coating and AlTiN-WC/C coating.

For the force and cutting energy are obtained by cutting tools with the same geometries under the same cutting conditions. The main factor that causes variations is the friction state between tool and chip. As can be seen in Figure 2, the AlTiN-WC/C multilayer coatings get lower friction force than other coatings. The WC/C soft coating can form a solid lubrication film on the tool surface. Chips are easy to move away against the coating, reducing the cutting force and total cutting energy. The AlTiN (67:33) coating also performs well, it may be because this coating forms a dense Al_2O_3 oxide film which of the tool rake face. This film prevents further oxidation of the coating and protect the tool at high temperature. The AlTiN (50:50) coating holds higher cutting force and cutting energy than that of other coatings, indicating that with this Al content, the performance of the coating is undesirable. Coatings fails and are peeled off, then chips stick on the rake face, increasing the cutting force and accelerating tool wear.

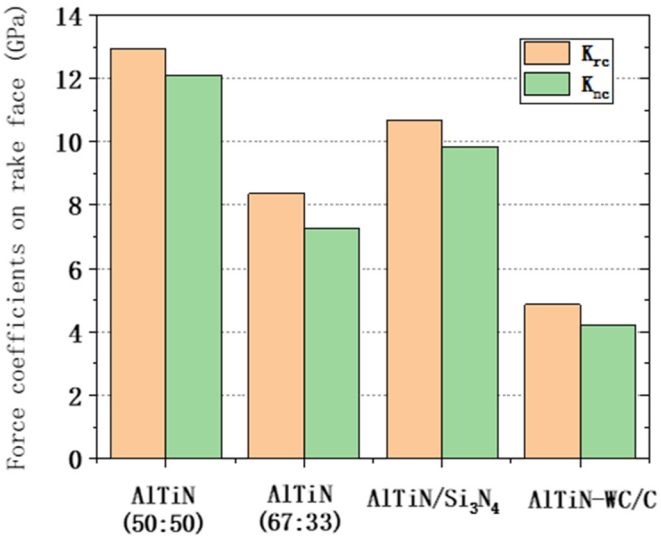


Figure 2. Force coefficients on rake face.

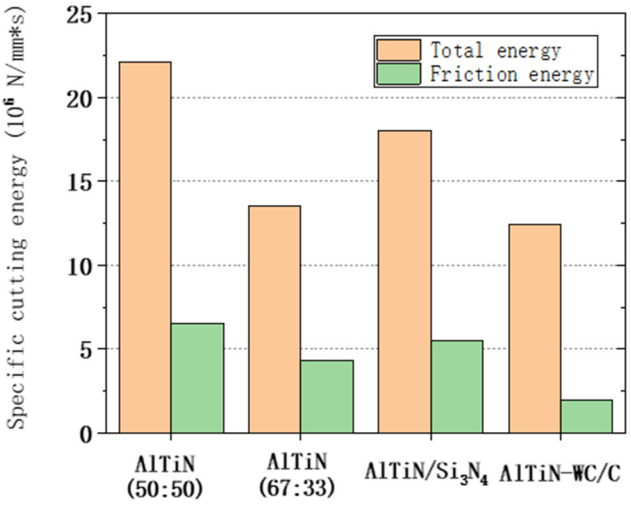


Figure 3. Specific cutting energy.

3.2. Milling Temperature

In this section, semi-artificial thermocouple method is used to measure the temperature of the cutting zone. A thin constantan wire is implanted between two SKD11 specimens and kept insulated from them. During milling, the constantan wire and SKD11 are cut off and form a thermal contact to generate voltage signals. In one turn of temperature measurement, the milling cutter cuts off constantan wire several times while moving forward, corresponding to the collection of multiple signal peaks. The number of multiple signal peaks is calculated theoretically as follows:

$$N = (R \sin \phi_c - f_z)/f_z \tag{4}$$

where, R is radius of the cutter, ϕ_c is contact angle, f_z is feed per tooth.

Figure 4 shows the obtained signal of milling temperature, in which the ordinate is the output voltage of thermocouple, and the corresponding milling temperature is calculated according to the calibration result of the SKD11–constantan wire thermocouple.

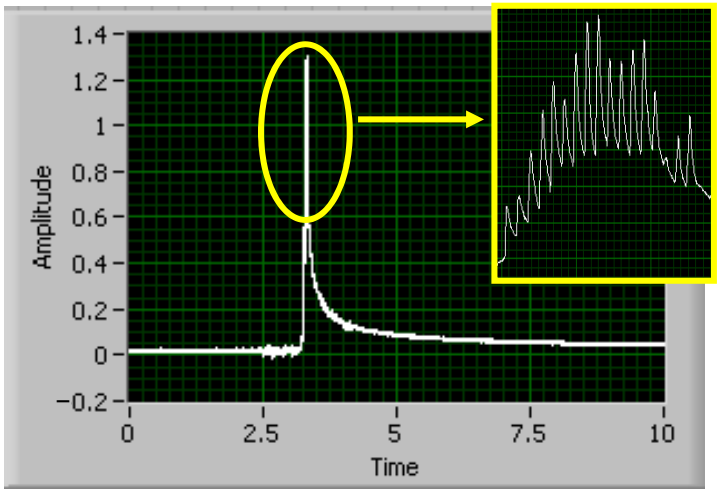


Figure 4. Signal of milling temperature.

Figure 5 shows that the cutting temperature varies when different coatings are applied. The highest cutting temperature among the tested cutters is 460 °C which is produced by AlTiN-WC/C coating while the lowest cutting temperature is about 300 °C obtained by the AlTiN (50:50) coating. The cutting temperature of 390 °C by the AlTiN (67:33) coating

and 350 °C by the AlTiN/Si_3N_4 coating fall in between. The temperature of the machined surface depends on the heat produced by shearing and friction in deformed regions and the thermal conductivity of cutters and workpiece materials. Heat generated by cutting can be approximately equal to the cutting energy consumed which has been discussed in the previous section. Due to the same substrate material of the milling cutter, the difference of thermal conductivity of the cutters is mainly caused by the coatings. For lower thermal conductivity of the coating, less heat is taken away and the temperature of the workpiece will rise. It can be seen that the cutting temperature of AlTiN-WC/C coating is higher than that of other tools, followed by AlTiN (67:33) coating and AlTiN/Si_3N_4 coating, and the temperature of AlTiN (50:50) coated tools is the lowest. Considering the order of specific cutting energy discussed in the last section, the higher milling temperature of AlTiN-WC/C-coated cutters and AlTiN (67:33)-coated cutters should be attributed to the lower thermal conductivity of the coating. With a lower thermal conductivity of the coating, the coating provides good insulation against the large amount of cutting heat generated by dry milling, resulting in more heat transfer to the workpiece and the chips.

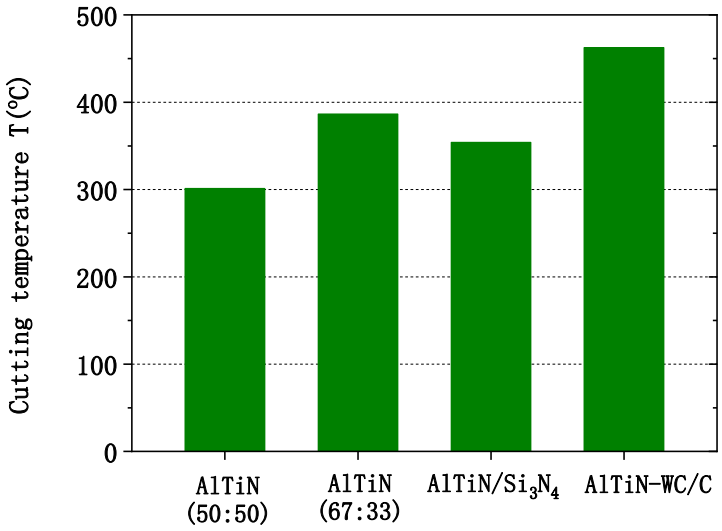


Figure 5. Milling temperature by different cutters.

During hard milling process with high cutting speed, high cutting temperature usually being one prominent cause which leads to poor surface quality and rapid tool failure. Reasonable cutting parameters should be applied to make the cutting temperature under the service temperature of coatings so that the coatings maintain good hardness and bonding strength while the hardened steel is softened. The cutting temperature obtained in this experiment test is between 300 °C to 500 °C, lower than the maximum service temperature for AlTiN coating and AlTiN-based composite coatings. As for the workpiece material SKD11, this cutting temperature is a medium tempering temperature that helps to soften the material. In this case, high cutting temperature is a benefit for reducing and slowing down the tool wear process.

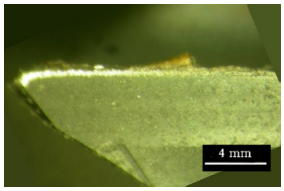
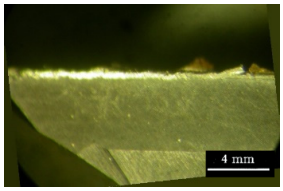
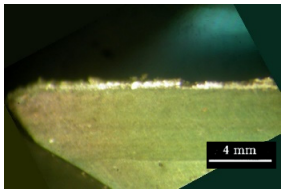
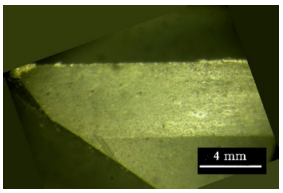
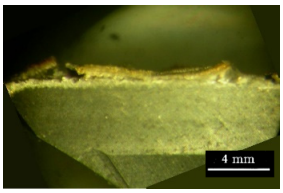
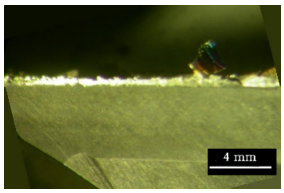
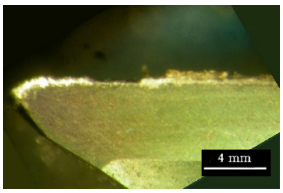
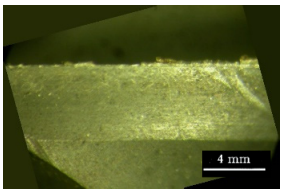
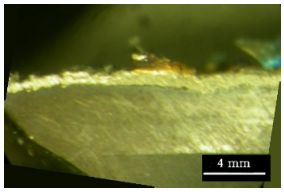
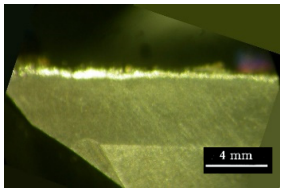
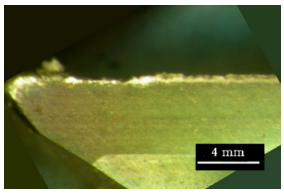
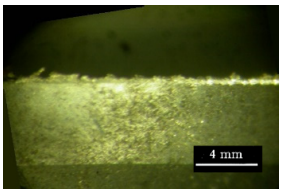
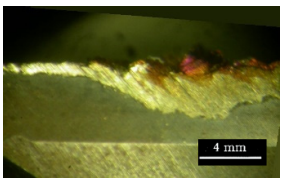
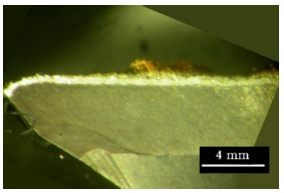
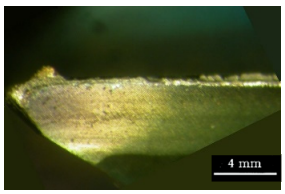
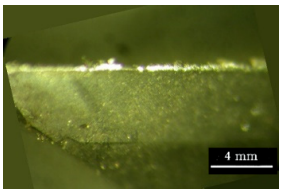
3.3. Tool Wear

In a hard-cutting process, tool edges are exposed to very heavy thermal and mechanical loads, Besides, due to the intermittent cut of rotating milling edge, the thermal mechanical load turns to be high-frequency impact, which is easy to cause fatigue failure of the cutters. The wear performance is closely related to the hardness, the binding force between the tool substrate material and the coating, and the toughness of the coatings at high temperature.

Table 4 shows the worn edge morphology in the dry milling process. Serious adhesion wear of cutting edges has been observed in the experiments. Due to high content of

chromium of the work SKD11, chips are observed to stick on the cutting edge like a ductile material, even at the early stage of cutting. This phenomenon is directly influenced by the distribution of cutting temperature and force on the rake face. Due to the intense pressure between the tool face and chip, and the influence of high cutting temperature, the bottom of the chip is easy to weld on the rake face near the cutting edge. Coating and tool substrate materials would then be peeled off with the sticking material. Adhesion wear could be relieved by reducing high cutting temperature and heavy mechanical loads, and improvement of friction conditions between the tool and the chips.

Table 4. Worn edge morphology in the dry milling process.

Cutting Length	AlTiN (50:50)	AlTiN (67:33)	AlTiN/Si_3N_4	AlTiN-WC/C
0.8 m				
1.6 m				
2.4 m				
3.2 m				

AlTiN (67:33) coating performs better than AlTiN (50:50) coating. On one hand, the aluminum-rich AlN phase in the coating has excellent mechanical properties, good bonding strength and good wear resistance in the machining process. On the other hand, with a high aluminum content in the coating, high temperature generated by the cutting causes the aluminum element to diffuse outward and combine with the oxygen in the air, and it is easy to form a dense Al_2O_3 oxide film, which can effectively prevent the further oxidation of the coating.

AlTiN/Si_3N_4 nanocomposite coating has a fine surface finish, which reduces the friction between tool and chip, and thus protects the tool from chip adhesions. In addition, nano-structure improves the toughness of the coating and thus enhances the resistance to high-frequency impact caused by intermittent cuts of the rotating milling edge.

AlTiN-WC/C multilayer coatings performed well in the test. Good lubrication features of WC/C coatings prevents the chip adhesive on the edges. WC/C coating on the outer layer can form a solid lubrication film on the tool surface which has a low shear strength, therefore chips easily take away WC/C film on the surface instead of sticking on the

coating. At the same time, AlTiN-WC/C coating also has good high temperature resistance as observed in the last section, which protects the tool from the high milling temperature.

Figure 6 shows the SEM micrographs of worn cutting edge with AlTiN (67:33) coating. Table 5 shows the elemental composition at scanning area P1 and P2. P1 is a coating area near the tip of the edge, where heavy adhesive chips are observed. P1 is the typical die steel components, showing that the chip materials also covered the coating nearby. There is no obvious diffusion or oxidation phenomenon. P2 is a coating area at the edge without much adhesion, where typical coating compositions and oxygen are found, showing the sign of oxidation. An Al_2O_3 film might be formed in the cutting at high temperature. Micro-chipping was found to be distributed along the cutting edge, which could be due to the falling of adhesive chips and the fatigue fracture under the periodic impact of heat and force.

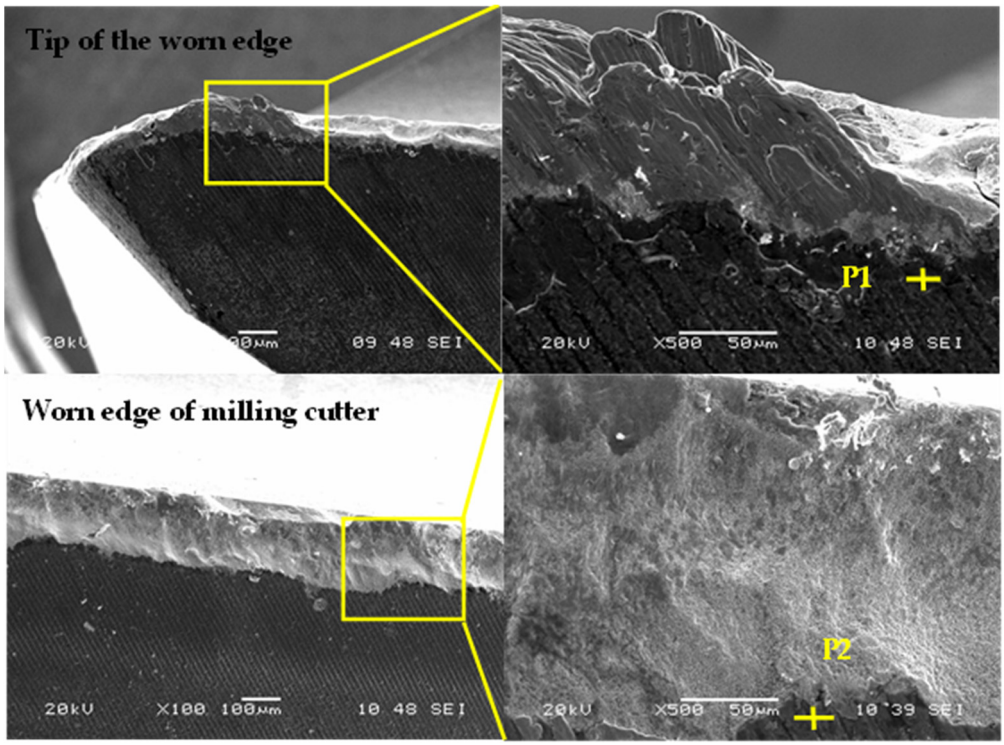


Figure 6. Micrographs of worn AlTiN (67:33) coated tool edge.

Table 5. Element components of P1 and P2 at wear land associated with Figure 6.

P1	Element	Wt%	At%	P2	Element	Wt%	At%
	CK	09.56	35.21		NK	06.35	13.50
	CrK	11.60	09.87		OK	13.64	25.38
	FeK	65.13	51.61		AlK	24.41	26.93
	WL	13.72	03.30		SiK	02.10	02.23
					TiK	38.72	24.07
					MnK	01.87	01.01
					FeK	12.91	06.88

3.4. Surface Integrity

To use hard milling in the finishing machining of dies and molds as an alternative to the traditional EDM and grinding process, the surface integrity in milling is considered one of the most important indices. During machining, the surface layer suffers high mechanical loads and thermal loads and even phase transformation which might lead to changes of surface quality. In the complex plastic deformation, and the grain is elongated, twisted and broken. This prevents further plastic deformation and strengthens the metal, increasing its

hardness and strength, as so called work hardening. On the other hand, high cutting temperature trends to soften the metal, and even cause phase change, which lead to the descend of hardness. The hardness of machined surface is the result of strengthening, weakening and phase transformation. Figure 7 shows the hardness of the machined surface. It can be seen that the hardness of machined surfaces by the tested coated cutters falls between 55 HRC and 59 HRC, lower than the original hardness (60–62 HRC). No obvious difference is observed in the surface hardness by tools with different coatings. This indicates that a softening effect induced by the high temperature dominates. The high temperature of hard cutting causes a certain degree of tempering to the surface material and weakens the hardness. As the tool wear increases, the cutting temperature increases, which intensifies the weakening trend of machined surface.

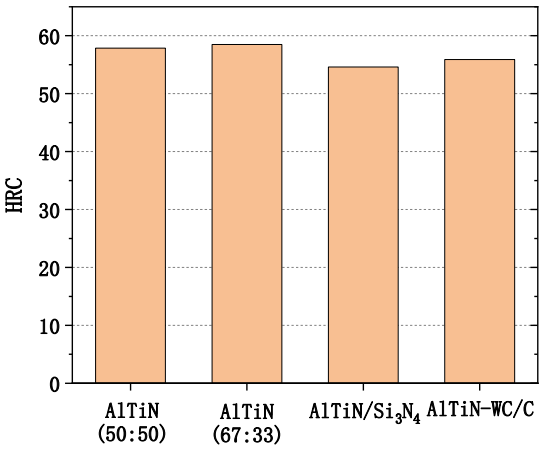


Figure 7. Hardness of machined surface.

Residual stress is also the result of force, heat and phase transition. The residual stress on the machined surface of each tool is shown in Figure 8. The residual stress measurements are carried out in direction X and direction Y, respectively. Direction X is the direction of tool feed and direction Y is perpendicular to the direction of tool feed. Hard milling of this hardened steel generates compressive stress in both directions on the machined surface, and the influence of coatings of cutting tool on the residual stress is not obvious. It is found in the experiments that the dry milling of hardened steel gains a quite satisfactory surface quality with proper tool wear condition. With the increase of tool wear, the surface quality deteriorated. This suggests that it should be avoided to use the tool with large wear to continue producing.

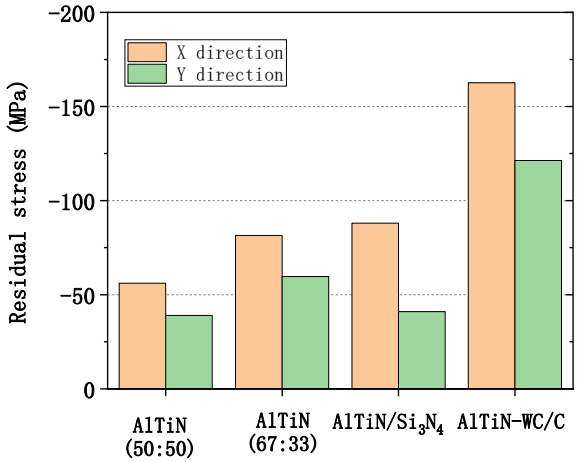


Figure 8. Residual stress of machined surface.

4. Conclusions

This study investigated the effects of the PVD AlTiN coatings and AlTiN-based composite coatings on cutting performance in dry milling of hardened steel SKD11. The friction force and pressure at the tool–chip interface, specific cutting energy, cutting temperature on the machined surface, tool wear pattern and mechanism, and surface integrity by AlTiN(50:50) coating, AlTiN(67:33) coating, AlTiN/Si_3N_4 coating and AlTiN-WC/C coating are studied and compared. The following conclusions are drawn:

1. The highest cutting force and cutting energy is produced by AlTiN (50:50) coating, followed by AlTiN/Si_3N_4 coating, AlTiN (67:33) coating and AlTiN-WC/C coating. Cutting force and cutting energy are effectively reduced by employing the coatings.

2. The highest cutting temperature among the tested cutters is 460 °C for AlTiN-WC/C coating, followed by 390 °C, 350 °C and 300 °C for AlTiN (67:33) coating, AlTiN/Si_3N_4 coating and AlTiN (50:50) coating respectively. High temperature helps to soften the workpiece while the good heat resistance of coatings protects the tool substrate so as to facilitate cutting.

3. The main wear mechanisms of the coated tools are adhesive wear, chipping induced by fatigue fracture and abrasive wear.

4. The hardness of machined surfaces decrease 2% to 12% than the original values. Compressive residual stress is induced on a machined surface. In general, the dry milling of hardened steel gains a quite satisfactory surface quality with proper tool wear conditions. Changes of coatings show no obvious influence on the hardness and the residual stress.

5. Compared with the other coatings, AlTiN-WC/C hard-soft multilayer coating performs better in reducing cutting force, preventing adhesion wear and isolating the cutting heat, being suitable for dry milling of hardened SKD11.

Author Contributions: Conceptualization, L.J. and Q.A.; methodology, L.J.; investigation, L.J. and Q.A.; resources, M.C.; writing—original draft preparation, L.J.; writing—review and editing, L.J. and Q.A.; project administration, M.C. All authors have read and agreed to the published version of the manuscript.

Funding: The work is supported by National Science and Technology Major Project (Y2019-VII-0018-0160).

Institutional Review Board Statement: Not applicable.

Informed Consent Statement: Not applicable.

Conflicts of Interest: The authors declare no conflict of interest.

References

1. Wang, C.; Ding, F.; Tang, D.; Zheng, L.; Li, S.; Xie, Y. Modeling and simulation of the high-speed milling of hardened steel SKD11 (62 HRC) based on SHPB technology. *Int. J. Mach. Tools Manuf.* **2016**, *108*, 13–26. [CrossRef]
2. Gong, F.; Zhao, J.; Jiang, Y.; Tao, H.; Li, Z.; Zang, J. Fatigue failure of coated carbide tool and its influence on cutting performance in face milling SKD11 hardened steel. *Int. J. Refract. Met. Hard Mater.* **2017**, *64*, 27–34. [CrossRef]
3. Gong, F.; Zhao, J.; Ni, X.; Liu, C.; Sun, J.; Zhang, Q. Wear and breakage of coated carbide tool in milling of H13 steel and SKD11 hardened steel. *SN Appl. Sci.* **2019**, *1*, 1111. [CrossRef]
4. Pimenov, D.Y.; Abbas, A.T.; Gupta, M.K.; Erdakov, I.N.; Soliman, M.S.; El Rayes, M.M. Investigations of surface quality and energy consumption associated with costs and material removal rate during face milling of AISI 1045 steel. *Int. J. Adv. Manuf. Technol.* **2020**, *107*, 3511–3525. [CrossRef]
5. Salur, E.; Kuntoğlu, M.; Aslan, A.; Pimenov, D.Y. The effects of MQL and dry environments on tool wear, cutting temperature, and power consumption during end milling of AISI 1040 steel. *Metals* **2021**, *11*, 1674. [CrossRef]
6. Lawal, S.; Choudhury, I.; Nukman, Y. Application of vegetable oil-based metalworking fluids in machining ferrous metals—A review. *Int. J. Mach. Tools Manuf.* **2012**, *52*, 1–12. [CrossRef]
7. An, Q.; Cai, C.; Zou, F.; Liang, X.; Chen, M. Tool wear and machined surface characteristics in side milling Ti6Al4V under dry and supercritical CO_2 with MQL conditions. *Tribol. Int.* **2020**, *151*, 106511. [CrossRef]
8. Javaroni, R.L.; Lopes, J.C.; Diniz, A.E.; Garcia, M.V.; Ribeiro, F.S.F.; Tavares, A.B.; Talon, A.G.; Sanchez, L.E.D.A.; de Mello, H.J.; Aguiar, P.R.; et al. Improvement in the grinding process using the MQL technique with cooled wheel cleaning jet. *Tribol. Int.* **2020**, *152*, 106512. [CrossRef]
9. Gajrani, K.K.; Suvin, P.S.; Kailas, S.V.; Rajurkar, K.P.; Sankar, M.R. Machining of hard materials using textured tool with minimum quantity nano-green cutting fluid. *CIRP J. Manuf. Sci. Technol.* **2021**, *35*, 410–421. [CrossRef]

10. Sankaranarayanan, R.; Rajesh Jesudoss Hynes, N.; Senthil Kumar, J.; Krolczyk, G.M. A comprehensive review on research developments of vegetable-oil based cutting fluids for sustainable machining challenges. *J. Manuf. Process.* **2021**, *67*, 286–313. [CrossRef]
11. Ramirez, C.; Ismail, A.I.; Gendarme, C.; Dehmas, M.; Aeby-Gautier, E.; Poulachon, G.; Rossi, F. Understanding the diffusion wear mechanisms of WC-10%Co carbide tools during dry machining of titanium alloys. *Wear* **2017**, *390–391*, 61–70. [CrossRef]
12. Krolczyk, G.; Maruda, R.; Krolczyk, J.; Wojciechowski, S.; Mia, M.; Nieslony, P.; Budzik, G. Ecological trends in machining as a key factor in sustainable production—A review. *J. Clean. Prod.* **2019**, *218*, 601–615. [CrossRef]
13. Klocke, F.; Eisenblätter, G. Dry cutting. *CIRP Ann.* **1997**, *46*, 519–526. [CrossRef]
14. Yuan, J.; Fox-Rabinovich, G.S.; Veldhuis, S.C. Control of tribofilm formation in dry machining of hardened AISI D2 steel by tuning the cutting speed. *Wear* **2018**, *402–403*, 30–37. [CrossRef]
15. Thakur, A.; Gangopadhyay, S. Dry machining of nickel-based super alloy as a sustainable alternative using TiN/TiAlN coated tool. *J. Clean. Prod.* **2016**, *129*, 256–268. [CrossRef]
16. Kumar, A.; Bauri, R.; Naskar, A.; Chattopadhyay, A. Characterization of HiPIMS and DCMS deposited TiAlN coatings and machining performance evaluation in high speed dry machining of low and high carbon steel. *Surf. Coat. Technol.* **2021**, *417*, 127180. [CrossRef]
17. Fujii, Y.; Imai, T.; Miyamoto, Y.; Ueda, N.; Hosoo, M.; Harigai, T.; Suda, Y.; Takikawa, H.; Tanoue, H.; Kamiya, M.; et al. Dry machining of metal using an engraving cutter coated with a droplet-free ta-C film prepared via a T-shape filtered arc deposition. *Surf. Coat. Technol.* **2016**, *307*, 1029–1033. [CrossRef]
18. Cavaleiro, D.; Figueiredo, D.; Moura, C.W.; Cavaleiro, A.; Carvalho, S.; Fernandes, F. Machining performance of TiSiN(Ag) coated tools during dry turning of TiAl6V4 aerospace alloy. *Ceram. Int.* **2021**, *47*, 11799–11806. [CrossRef]
19. Arndt, M.; Kacsich, T. Performance of new AlTiN coatings in dry and high speed cutting. *Surf. Coat. Technol.* **2003**, *163–164*, 674–680. [CrossRef]
20. PalDey, S.; Deevi, S.C. Single layer and multilayer wear resistant coatings of (Ti,Al)N: A review. *Mater. Sci. Eng. A* **2003**, *342*, 58–79. [CrossRef]
21. He, Q.; DePaiva, J.M.; Kohlscheen, J.; Beake, B.D.; Veldhuis, S.C. Study of wear performance and tribological characterization of AlTiN PVD coatings with different Al/Ti ratios during ultra-high speed turning of stainless steel 304. *Int. J. Refract. Met. Hard Mater.* **2021**, *96*, 105488. [CrossRef]
22. Lian, Y.; Long, Y.; Zhao, G.; Mu, C.; Li, X.; Deng, J.; Xie, C. Performance of CrCN-WS_2 hard/soft composite coated tools in dry cutting of titanium alloys. *J. Manuf. Process.* **2020**, *54*, 201–209. [CrossRef]
23. Kumar, C.S.; Majumder, H.; Khan, A.; Patel, S.K. Applicability of DLC and WC/C low friction coatings on Al_2O_3/TiCN mixed ceramic cutting tools for dry machining of hardened 52100 steel. *Ceram. Int.* **2020**, *46*, 11889–11897. [CrossRef]
24. Benedetti, M.; Fontanari, V.; Torresani, E.; Girardi, C.; Giordanino, L. Investigation of lubricated rolling sliding behaviour of WC/C, WC/C-CrN, DLC based coatings and plasma nitriding of steel for possible use in worm gearing. *Wear* **2017**, *378–379*, 106–113. [CrossRef]
25. Vera, E.; Vite, M.; Lewis, R.; Gallardo, E.; Laguna-Camacho, J. A study of the wear performance of TiN, CrN and WC/C coatings on different steel substrates. *Wear* **2011**, *271*, 2116–2124. [CrossRef]
26. Liu, Z.; An, Q.; Xu, J.; Chen, M.; Han, S. Wear performance of (nc-AlTiN)/(a-Si_3N_4) coating and (nc-AlCrN)/(a-Si_3N_4) coating in high-speed machining of titanium alloys under dry and minimum quantity lubrication (MQL) conditions. *Wear* **2013**, *305*, 249–259. [CrossRef]
27. Zhang, S.; Wu, W.; Chen, W.; Yang, S. Structural optimisation and synthesis of multilayers and nanocomposite AlCrTiSiN coatings for excellent machinability. *Surf. Coat. Technol.* **2015**, *277*, 23–29. [CrossRef]
28. Uhlmann, E.; Fuentes, J.O.; Gerstenberger, R.; Frank, H. nc-AlTiN/a-Si_3N_4 and nc-AlCrN/a-Si_3N_4 nanocomposite coatings as protection layer for PCBN tools in hard machining. *Surf. Coat. Technol.* **2013**, *237*, 142–148. [CrossRef]
29. Shaw, M.C.; Cookson, J. *Metal Cutting Principles*; Oxford University Press: New York, NY, USA, 2005.
30. Altintas, Y. *Manufacturing Automation-Metal Cutting Mechanics, Machine Tool Vibrations and CNC Design*, 2nd ed.; Cambridge University Press: New York, NY, USA, 2012.